

UNIVERSAL ABSTRACTION: HARNESSING FRONTIER MODELS TO STRUCTURE REAL-WORLD DATA AT SCALE

Cliff Wong^{1*}, Sam Preston^{1*}, Qianchu Liu^{1*}, Zelalem Gero¹, Jaspreet Bagga¹, Sheng Zhang¹,
Shrey Jain¹, Theodore Zhao¹, Yu Gu¹, Yanbo Xu¹, Sid Kiblawi¹, Srinivasan Yegnasubramanian⁷,
Taxiarchis Botsis⁷, Marvin Borja⁷, Luis M. Ahumada⁷, Joseph C. Murray⁷, Guo Hui Gan^{2,5},
Roshanthi Weerasinghe⁴, Kristina Young^{5,6}, Rom Leidner^{3,5}, Brian Piening^{3,5}, Carlo Bifulco^{3,5},
Tristan Naumann¹, Mu Wei^{1†}, and Hoifung Poon^{1†}

¹Microsoft Research, Redmond, WA, USA

²Providence Portland Medical Center, Portland, OR, USA

³Providence Genomics, Portland, OR, USA

⁴Providence Research Network, Renton, WA, USA

⁵Earle A. Chiles Research Institute, Providence Cancer Institute, Portland, OR, USA

⁶The Oregon Clinic, Radiation Oncology Division, Portland, OR

⁷Johns Hopkins University School of Medicine, Baltimore, MD, USA

*Equal contributions

†Corresponding authors: muhsin.wei@microsoft.com, hoifung@microsoft.com

ABSTRACT

A significant fraction of real-world patient information resides in unstructured clinical text. Medical abstraction extracts and normalizes key structured attributes from free-text clinical notes, which is the prerequisite for a variety of important downstream applications, including registry curation, clinical trial operations, and real-world evidence generation. Prior medical abstraction methods typically resort to building attribute-specific models, each of which requires extensive manual effort such as rule creation or supervised label annotation for the individual attribute, thus limiting scalability.

In this paper, we show that existing frontier models already possess the “universal abstraction” capability for scaling medical abstraction to a wide range of clinical attributes. We present UNIMEDABSTRACTOR (UMA), a unifying framework for zero-shot medical abstraction with a modular, customisable prompt template and the selection of any frontier large language models (LLMs). Given a new attribute for abstraction, users only need to conduct lightweight prompt adaptation in UMA to adjust the specification in natural languages. Compared to traditional methods, UMA eliminates the need for attribute-specific training labels or hand-crafted rules, thus substantially reducing the development time and cost.

We conducted a comprehensive evaluation of UMA in oncology using a wide range of marquee attributes representing the cancer patient journey. These include relatively simple attributes typically specified within a single clinical note (e.g., performance status, treatment), as well as complex attributes requiring sophisticated reasoning across multiple notes at various time points (e.g., tumor site, histology, staging). Based on a single frontier model such as GPT-4o, UMA matched or even exceeded the performance of state-of-the-art attribute-specific methods, each of which was tailored to the individual attribute. To facilitate population-scale real-world data structuring and evidence generation, we will release our code at https://github.com/microsoft/ua_oncophenotype.

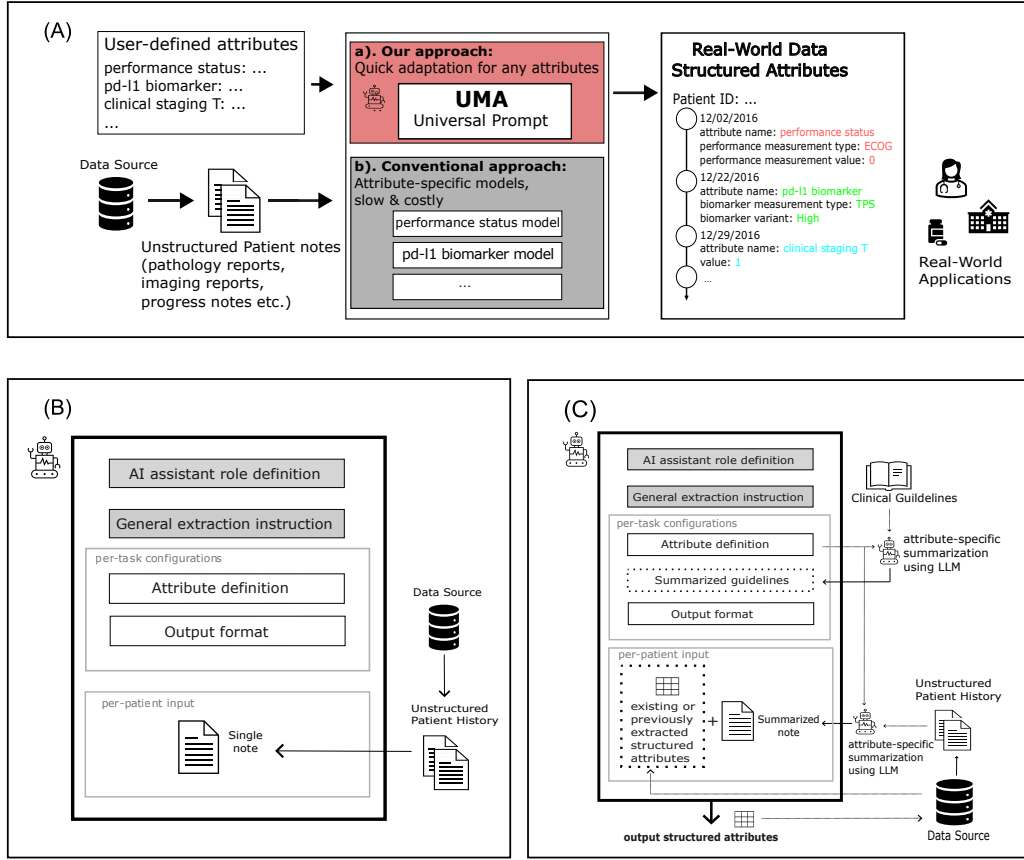


Figure 1: (A): Overview of UNIMEDABTRACTOR (UMA), a one-model-for-all universal abstraction method for medical attribute abstraction. In contrast with conventional approaches that build specialized models for each specific attribute (slow and costly due to the manual collection of training labels or heuristic rules), UMA can be quickly configured to abstract any user-defined medical attributes from unstructured patient data in a zero-shot manner. The outcome of the pipeline is structured real-world data that serves as the foundation for real-world applications such as clinical trial matching, data curation for surveillance and monitoring, drug discovery, etc. (B) UMA instantiation template for short-context attributes which can be extracted from within a single note (an example prompt is in Figure 4). (C) UMA instantiation template for long-context attributes (e.g. cancer staging attributes) which require complex reasoning over multiple notes and long clinical guidelines (an example prompt is in Figure 5). We also provide the flexibility to chain the prompts to leverage previously extracted attributes.

1 INTRODUCTION

Real-world data (RWD) in healthcare refers to information collected from records representing standard medical care as opposed to data from research clinical trials. RWD can offer a more comprehensive view of patient experiences, helps optimize healthcare delivery, and supports more informed decision-making across the healthcare ecosystem. Particularly, RWD can be used to generate real-world evidence (RWE) which is increasingly utilized for medical evidence generation, providing a complement to the existing standard use of a randomized controlled trial (RCT). A significant proportion of RWD comes from unstructured patient data, such as dictated progress notes and radiology reports, which store much of the patient information needed to improve care and clinical research. Medical abstraction is a process that structures RWD by extracting and normalizing information from unstructured patient records. Traditional medical abstraction methods for structuring RWD still require substantial manual efforts, such as crafting extraction rules or annotating examples for

supervised learning. These manual efforts are expensive and time-consuming. In the U.S. alone, there are close to two million new cancer patients each year and curating key information for a single patient takes hours. As such, traditional abstraction is a significant barrier to realizing the full opportunity presented by the digitization of medical records (Rudrapatna et al., 2020). Moreover, evolving guidelines for defining key cancer attributes further compounds the challenge, leading to semantic drift and therefore often rendering previously collected labels outdated Gao et al. (2021; 2019); Preston et al. (2023b).

While traditional methods face challenges in efficiently scaling up medical abstraction due to the need to develop specialized models for each specific attribute, state-of-the-art large language models (LLMs) such as GPT-4o have demonstrated emergent capabilities in biomedical applications without requiring any specialized training Lee et al. (2023); Nori et al. (2023). In this paper, we propose UNIMEDABTRACTOR (UMA), a framework that harnesses the universal structuring capabilities of LLMs for zero-shot universal abstraction. Here we define universal abstraction as a one-model-for-all approach that can efficiently scale to extract new attributes from any ontology, adapt to evolving guidelines, and handle new patients and datasets across different institutions. The key to UMA is a modular template that can flexibly incorporate patient data and the user-defined task definitions for each attribute. UMA can also accommodate different types of input (single note, multiple notes, long guidelines, etc.) and requirements for abstracting different types of attributes (Figure 1A).

We test UMA in oncology, where medical abstraction is particularly challenging. Our main experiments are conducted on real-world data from the Providence Health System, a large integrated delivery network. Without requiring any specialized training, UMA displays impressive universal abstraction capabilities. UMA with GPT-4o surpasses conventional baselines in the overall performance by around 2 absolute points in F1/accuracy scores. Its performance further improves on the more challenging long-context attribute abstraction tasks when using the advanced reasoning model O1. In some cases, such as pathologic T in cancer staging, UMA even outperforms the supervised method by over 20 absolute points in accuracy. We also demonstrate that UMA generalizes more effectively than supervised models. Evaluated on a comparable real-world dataset from another institution (Johns Hopkins), UMA shows greater robustness to distributional shifts. Additionally, UMA achieves a substantial reduction in cost and human labor, cutting both to less than one-tenth of the conventional approach.

2 UNIVERSAL ABSTRACTION WITH UMA

We propose UMA (pronounced as ['u:ma']), a universal abstraction framework to leverage large language models to structure real world data from unstructured patient notes in a zero-shot manner. UMA uses a flexible prompt template that allows users to specify target attributes, combining pre-defined components, task-specific configurations, and per-patient inputs. It also includes advanced modules to support complex, long-context attributes requiring long-term reasoning. An overview of the template is shown in Figure 1B and Figure 1C.

2.1 PRE-DEFINED: GENERAL TASK INTRODUCTION

We begin by providing the LLM with a general understanding of the medical abstraction task, enabling broad applicability across attributes. The universal prompt template starts with predefined, generic instructions that frame the task as event extraction, where each event group corresponds to an attribute occurrence in the patient record. Each group contains specific descriptors that characterize the event. This setup allows users to later specify attribute definitions, relevant descriptors, and expected outputs for each occurrence.

2.2 ATTRIBUTE-SPECIFIC TASK CONFIGURATIONS

We modularize the task configurations to ensure scalability for new attributes. For each attribute, we configure the following components:

Attribute definition For each task, we set up an attribute definition block in the prompt where the user can specify the attribute’s meaning, relevant descriptors, and expected output formats—e.g., verbatim text or predefined categories. For example, the performance status attribute may include:

```
"performance status measurement type":
  name of measurement type: ECOG, KPS, PPS, or Lansky
"performance status value":
  the measured value of performance status measurement type.
  Extract only the numerical value.
```

To improve interpretability and accuracy, users can also define contextual descriptors (e.g., note date, certainty, source spans, model reasoning), which aid both postprocessing and guiding the LLM toward correct outputs (see ablation results in Figure 3).

Output format To streamline extraction and post-processing, outputs are formatted as a list of JSON objects, with each representing an attribute occurrence. We provide an output template to guide the LLM, where each dictionary maps descriptor names to values extracted from the text. For example, the output format for performance status is:

```
[
  {
    "performance status measurement type":
    <performance status type>,
    "performance status value":
    <performance status value>
  }
  ...
]
```

Long-context Attribute: Incorporating clinical guidelines Some tasks require integrating complex clinical guidelines, such as those from the ICD-O (240+ pages) or AJCC Cancer Staging Manual (600+ pages). Due to LLM context limitations, directly including these guidelines is impractical. To address this, we perform a one-time structuring of the guidelines using GPT-4 to generate attribute-specific summaries. By incorporating the attribute definition block into the summarization prompt, we ensure relevance and efficiency in guiding the model (see Figure 1C).

2.3 PATIENT INPUT

Once the prompt template is configured, patient data—typically unstructured text from sources like pathology, imaging, surgical, or progress notes—is provided as input. The template is designed to flexibly accommodate any note type.

Long-context Attributes: Reasoning Across Patient History For tasks requiring longitudinal reasoning, inserting individual notes is insufficient. Patients often have 20+ notes spanning their clinical history. To handle this, we apply GPT-4 to perform attribute-specific summarization across notes, generating a concise, chronological patient summary (see Figure 1C).

This approach reduces input length, cuts computational costs and latency, and improves performance by eliminating duplicated or irrelevant content—long known to impair LLM quality Searle et al. (2021); Liu et al. (2024); Mirzadeh et al. (2024). We demonstrate the impact of this summarization in our ablation studies (Figure 3).

Long-context Attribute: Leveraging Structured Data The prompt template includes an optional block to incorporate existing or previously extracted structured data alongside unstructured input. This contextual information can narrow the focus of extraction and improve accuracy. For example, knowing the treatment date helps restrict clinical staging to pre-treatment notes, and providing the tumor site can aid staging attribute extraction.

Postprocessing Thanks to its modular design, integrating UMA into the attribute abstraction pipeline is seamless. After obtaining the JSON output from the LLM, we apply post-processing to refine and finalize the extracted attributes. Descriptors in the output can be used to filter for high-quality occurrences—for example, excluding non-cancerous events based on a disease type descriptor improves precision in response extraction.

Extracted values are then normalized to standard medical ontologies (e.g., ICD-10-CM, NCI Thesaurus, HGNC, HGVS) or to numerical lab values. We use heuristics to expand synonyms for each entity and apply string matching for normalization.

To reduce redundancy, duplicate values across or within notes with similar timestamps are merged into a single attribute group. Each occurrence is then linked to the patient ID and note timestamp where applicable, enabling timeline construction for downstream applications.

3 TASKS AND EXPERIMENT SETUP

As a testbed, we apply UMA to abstract a representative set of oncology attributes, spanning both short-context attributes—extractable within a single note—and long-context attributes that require reasoning over longitudinal records and complex clinical guidelines. Short-context attributes include PD-L1, performance status, treatment, response, progression, and case finding. Long-context attributes include coarse- and fine-grained primary site, histology, and clinical/pathologic T, N, and M stages. A full list of attributes and their associated descriptors is provided in Table S1.

Datasets were drawn from two health systems—Johns Hopkins and Providence—and comprise diverse patient documents. Attribute-specific datasets vary based on the availability of manual ground-truth annotations (see Tables S2 and S3). Long-context labels were obtained from cancer registries, while short-context labels were curated in collaboration with Providence clinicians.

All UMA experiments are conducted in a zero-shot setting without training labels. For optimal performance, we use state-of-the-art LLMs, including GPT-4 and GPT-4o (version: 2024-05-13). For long-context tasks requiring complex reasoning, we additionally evaluate O1 (version: 2024-12-17). Where training labels exist, we compare against BERT-based supervised baselines. In their absence, we report heuristic baselines based on domain-specific rules from González et al. (2023). We report F1 scores for short-context attributes and accuracy for long-context attributes.

Further dataset and experimental details are available in Section 10.1 and Section 10.2.

4 EXPERIMENTAL RESULTS

4.1 SHORT-CONTEXT ATTRIBUTE ABSTRACTION

As shown in the top sub-figure in Figure 2, UMA with GPT-4o delivers the best overall performance across six short-context attribute abstraction tasks, achieving the best F1 score. We also observe an overall performance gain when moving from GPT-4 to GPT-4o, demonstrating that UMA effectively leverages improvements in base LLMs. Notably, for the PD-L1 biomarker and performance status abstraction tasks, UMA with GPT-4o already reaches ceiling performance. Across the individual tasks, UMA with GPT-4o either outperforms or matches the baseline apart from case finding where the supervised baseline is trained on tens of thousands of labels. It is worth highlighting that the human effort required to develop the case finding model far exceeds that of UMA. While the baseline model relies on over 10,000 hours of manual data curation, UMA requires less than an hour to define the attributes via prompt engineering. The strong overall performance and substantial cost savings of UMA make it a compelling alternative to traditional attribute extraction methods.

4.2 LONG-CONTEXT ATTRIBUTE ABSTRACTION: CANCER STAGING

The second sub-figures in Section 10.2 compare UMA and supervised baselines on long-context cancer staging abstraction tasks in the Providence dataset. Despite operating in a zero-shot setting¹, UMA outperforms the supervised model by over 2 absolute points in accuracy, including a 20-point

¹While full examples are not provided, some prompts include fixed snippets to clarify guideline application.

gain on the pathologic T attribute. Similar to short-context tasks, UMA benefits from advances in the underlying model—particularly with O1—showing notable improvements on complex, reasoning-heavy TNM attributes.

While UMA lags behind the supervised baseline on certain tasks such as fine-grained primary site, histology, and clinical T, its performance remains impressive given the setting. The supervised models were trained on split subsets of the same dataset (i.e. allowing them to learn dataset-specific annotation nuances) and required over 10,000 hours of manual labeling. In contrast, UMA relies on under an hour of prompt design, highlighting its efficiency and scalability.

A further limitation of supervised models is their dependence on labeled data, which is rarely available across all institutions. The third sub-figure in Figure 2 evaluates model generalizability by applying the Providence-trained supervised model and UMA to the Johns Hopkins dataset, which was only used for evaluation. Here, UMA significantly outperforms the supervised baseline, demonstrating greater robustness to distribution shifts and superior generalization. Unlike supervised models that risk overfitting to spurious correlations in training data, UMA relies solely on structured prompts grounded in clinical guidelines, making it a more reliable solution for deployment across diverse or unseen datasets.

To assess the contribution of key components in UMA, we conducted ablation studies on the summarization step and the use of evidence and reasoning descriptors in the attribute definition block (Figure 3). While summarization primarily addresses context length limitations, we evaluated its impact on performance using GPT-4-32k, which has a larger context window. Comparing two setups—one with summarization and one using concatenated full notes (restricted to patients within the 32k-token limit)—we found that summarization not only improves efficiency but also enhances accuracy, likely by filtering out irrelevant information. We also ablated the attribute definition prompt by removing the evidence and reasoning descriptors. This led to a performance drop, particularly on the breast cancer dataset, where abstraction tasks are more complex. These descriptors serve as grounding mechanisms, akin to chain-of-thought reasoning, and improve model accuracy on tasks requiring deeper inference.

5 DISCUSSION

5.1 THE POTENTIAL FOR UMA INTEGRATION INTO CLINICAL WORKFLOWS

The strong performance and rapid development cycle of UMA make it highly scalable for universal abstraction. Unlike conventional methods that require months or years to curate training data or craft heuristics, UMA enables near-instant onboarding of new attributes—limited only by the time needed to define them in prompts. This allows for fast, large-scale generation of structured patient records to support a wide range of downstream applications, from clinical decision support to trial recruitment. Moreover, UMA can easily accommodate evolving clinical guidelines, a critical feature as many now follow rolling updates. In cancer staging, for instance, different guideline versions must be applied based on diagnosis dates, a requirement UMA can seamlessly handle.

Despite UMA’s strong performance, clinical use still requires human oversight. UMA facilitates efficient review by producing interpretable outputs: summarized patient histories for context, evidence descriptors for traceability, and reasoning descriptors that explain model logic—serving as a built-in chain-of-thought. Additionally, UMA is well-suited for long-context abstraction tasks, where efficiency is paramount. Summarization not only improves token usage but also accelerates human review. In dynamic clinical settings, updated abstractions can be generated by summarizing new notes and appending them to existing summaries, enabling continuous, efficient updates to structured patient data.

5.2 LIMITATIONS

A key limitation of our study is data quality, particularly missing information due to the fragmented nature of patient records. Unlike cancer registries that aggregate data across providers, our dataset is confined to a single EHR system, limiting visibility into a patient’s full medical history. Future work should incorporate notes from multiple hospital systems and clinics to improve the completeness and accuracy of longitudinal patient data.

Additionally, this study serves as a proof-of-concept, showcasing the effectiveness of basic prompting with LLMs. While our simple approach already matches or outperforms conventional methods, we did not explore more advanced prompting strategies—such as self-verification, self-consistency, or few-shot learning—which could further improve performance. Evaluation of a broader range of LLMs, including open-source models like DeepSeek R1 and LLaMA, is also left for future work.

6 RELATED WORK

6.1 CONVENTIONAL APPROACHES TO AUTOMATE MEDICAL ABSTRACTION

Automated data extraction using NLP and machine learning has been widely explored in oncology. Gauthier et al. (2022) demonstrated that automated extraction from EHRs of advanced lung cancer patients was both accurate and faster than manual abstraction, despite challenges like unstructured text and non-standard terminology. Preston et al. (2023a) used registry-derived, patient-level supervision to train deep neural network models for cross-document extraction, achieving high performance on core tumor attributes and highlighting potential for accelerating registry curation. Kefeli et al. (2024) proposed a BERT-based model to classify TNM stages directly from pathology reports, using publicly available data.

6.2 LLMs IN MEDICAL ABSTRACTION

Recent studies have applied LLMs like GPT-4 to abstract clinical attributes from oncology notes, showing strong performance in tasks such as Named Entity Recognition and relation extraction Zhou et al. (2024); Bhattarai et al. (2024); Goel et al. (2023); Hu et al. (2024); Wong et al. (2023). These approaches typically use prompt engineering and few-shot learning to identify entity spans, types, and relationships. However, existing work lacks scalable prompting strategies for handling multiple attributes and end-to-end evaluation. Furthermore, little attention has been given to guideline-based classification and evidence aggregation across notes—gaps our study aims to address.

7 CONCLUSION

In this paper, we introduced UMA, a zero-shot and one-model-for-all framework that utilizes an underlying LLM to automate medical abstraction across multiple attributes from unstructured clinical notes. Through a flexible universal prompt template, UMA achieves universal abstraction in the way that it can easily generalize to different types of attributes (including both simple short-context and complex long-context oncology attributes) and can cope with long input, complex reasoning and involving guidelines. Compared with the conventional approaches that build attribute-specific models, UMA is a single model that is both more scalable with much lower adaptation costs for onboarding new attributes and achieving better overall performance. In particular, UMA improves generalizes significantly better than supervised baselines across different datasets from different institutions. We believe that UMA provides a promising direction for medical abstraction in the future with great potential to enhance the efficiency, scalability and usability in the clinical workflow.

8 HUMAN SUBJECTS/IRB, DATA SECURITY, AND PATIENT PRIVACY

This work was performed under institutional review board (IRB)-approved research protocols (Providence protocol ID 2019000204, Johns Hopkins protocol ID IRB00482075) and was conducted in compliance with human subjects research and clinical data management procedures—as well as cloud information security policies and controls—administered within Providence Health and Johns Hopkins Medicine. All study data were integrated, managed, and analyzed exclusively and solely on Providence-or Johns Hopkins-managed cloud infrastructure. All study personnel completed and were credentialed in training modules covering human subjects research, use of clinical data in research, and appropriate use of IT resources and IRB-approved data assets.

9 NOTES

We thank the inHealth Precision Medicine program, the Armstrong Institute Cancer Registry team, and the Sidney Kimmel Comprehensive Cancer Center Precision Medicine and Molecular Tumor Board groups at Johns Hopkins for their help and support in curating the Johns Hopkins dataset and providing guidance on evaluation of model performance. We also thank Providence Portland Medical Center, Providence Genomics, the Providence Research Network, the Providence Cancer Institute, and the Oregon Clinic for their assistance in curating and labeling the Providence dataset and guiding the evaluation process.

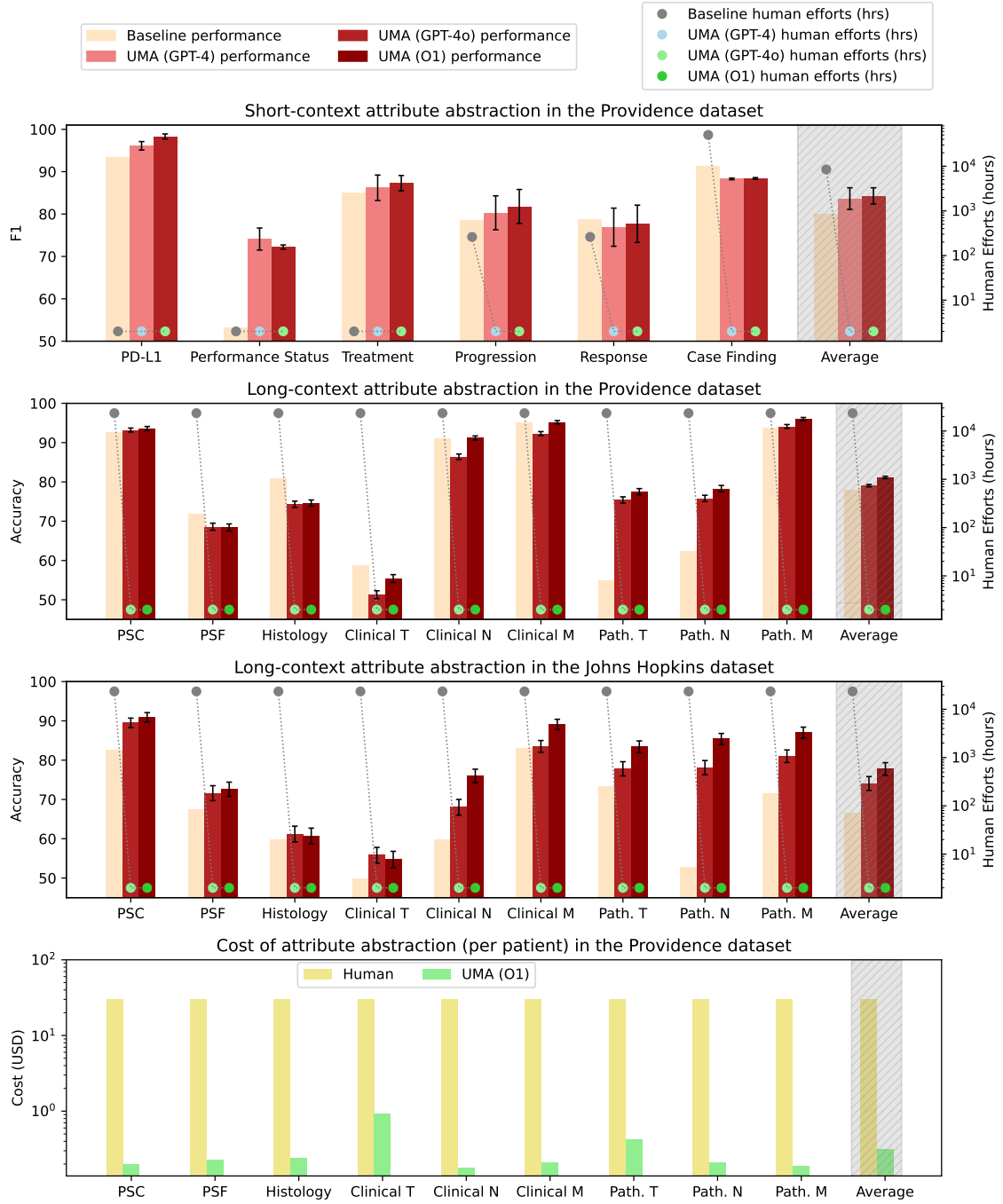


Figure 2: UMA main results. The top three sub-figures represent the performance on short-context attribute abstraction in Providence data and long-context attribute abstraction across both Providence and Johns Hopkins datasets. Standard deviation from 1000 bootstrapping sampling procedures is reported as error bars. Detail numbers are in Table S4, Table S5, and Table S6. All the baseline approaches are supervised baselines except for PD-L1, Performance Status and Treatment where the baseline approach is heuristics-based as no training data is available. The number of human hours involved are estimated from 1 hour per case as reported in (Miller et al., 2024). The last row represents the inference cost for UMA (O1) (also see Table S7) as compared with the cost of hiring humans to annotate the same testsets. Human annotation cost is approximated using the average hourly wage of a cancer registrar (30 USD/hour) (National Cancer Registrars Association, 2022). We show that UMA achieves an overall better performance across different attribute types and across different institutions with significant cost and human effort reduction compared with conventional baseline approaches for medical abstraction.

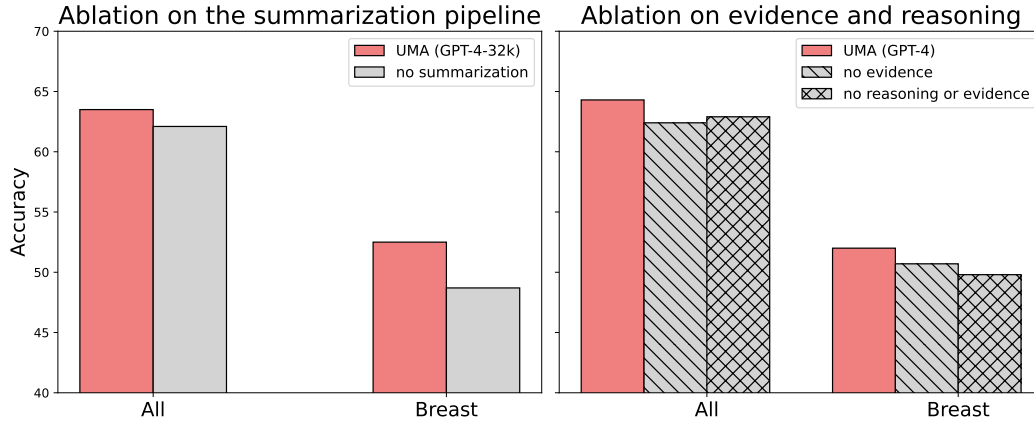


Figure 3: Ablating the key components (summarization, evidence, reasoning) in UMA for abstracting long-context attributes (fine-grained primary site) on the Providence dataset. “All” includes all tumor sites, while “Breast” includes only the more challenging abstraction tasks for ‘breast’ cancer patients.

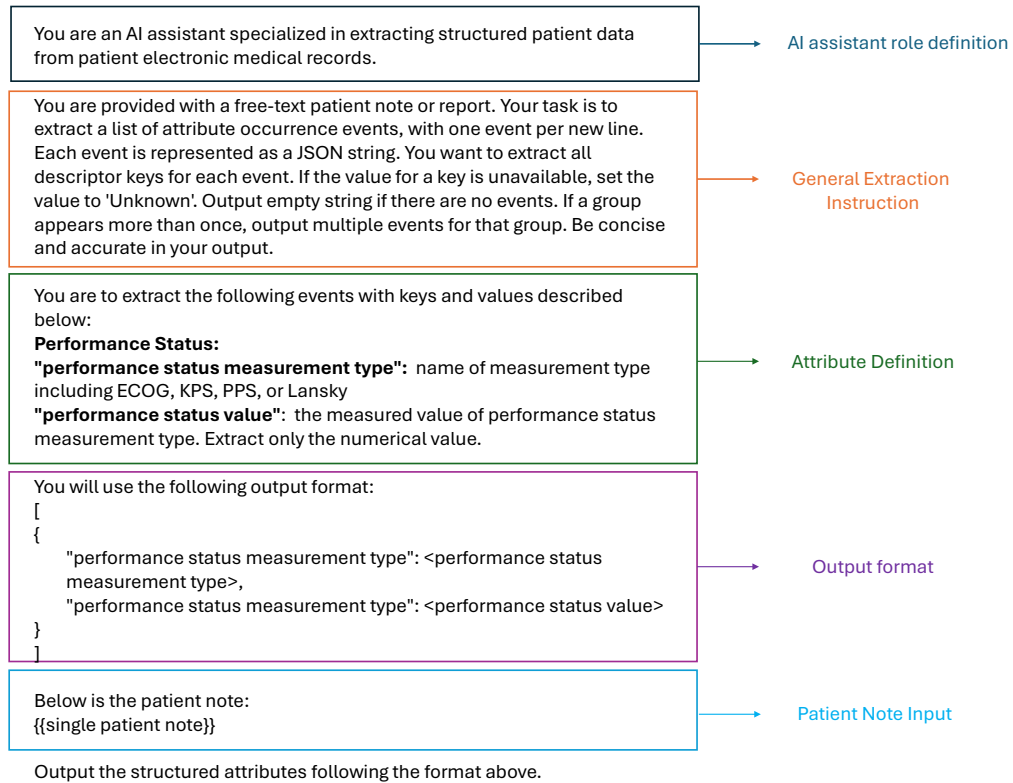


Figure 4: Example short-context attribute UMA prompt for extracting performance status from patient note

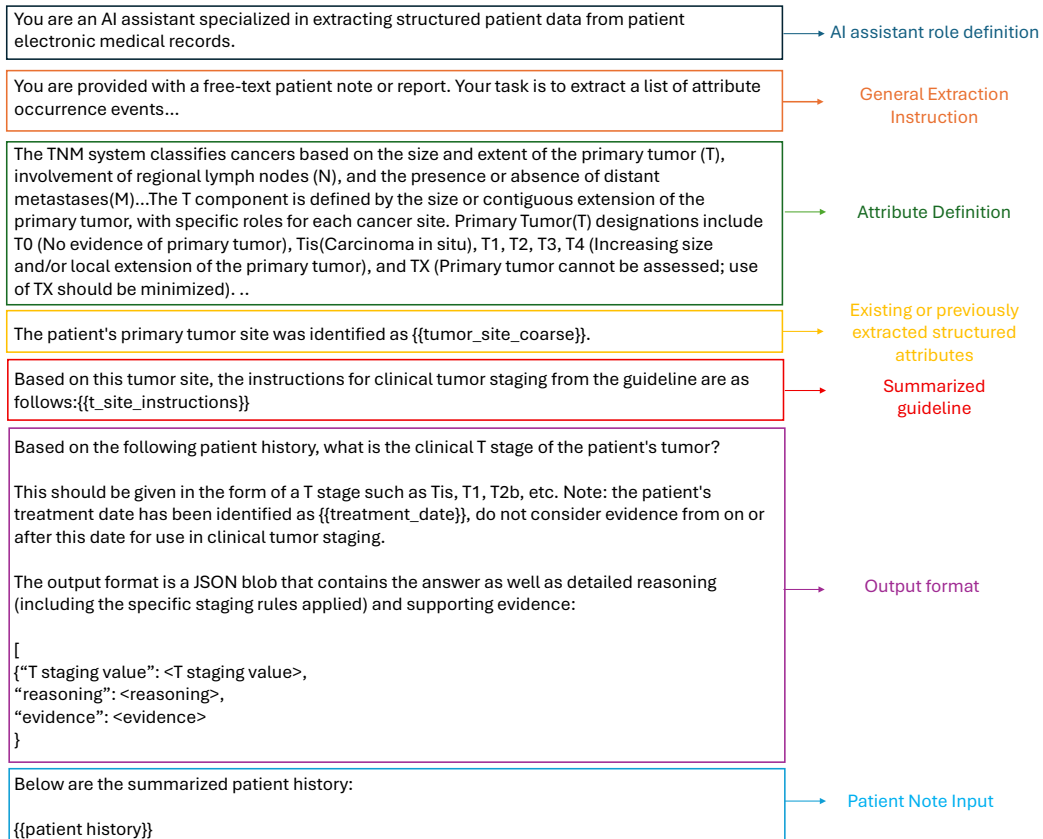


Figure 5: Example long-context attribute UMA prompt for extracting clinical staging T from a history of patient notes

REFERENCES

- Kriti Bhattacharai, Inez Y Oh, Jonathan Moran Sierra, Jonathan Tang, Philip RO Payne, Zach Abrams, and Albert M Lai. Leveraging gpt-4 for identifying cancer phenotypes in electronic health records: a performance comparison between gpt-4, gpt-3.5-turbo, flan-t5, llama-3-8b, and spacy's rule-based and machine learning-based methods. *JAMIA open*, 7(3):ooae060, 2024.
- Shang Gao, John X Qiu, Mohammed Alawad, Jacob D Hinkle, Noah Schaefferkoetter, Hong-Jun Yoon, Blair Christian, Paul A Fearn, Lynne Penberthy, Xiao-Cheng Wu, et al. Classifying cancer pathology reports with hierarchical self-attention networks. *Artificial intelligence in medicine*, 101:101726, 2019.
- Shang Gao, Mohammed Alawad, M Todd Young, John Gounley, Noah Schaefferkoetter, Hong Jun Yoon, Xiao-Cheng Wu, Eric B Durbin, Jennifer Doherty, Antoinette Stroup, et al. Limitations of transformers on clinical text classification. *IEEE journal of biomedical and health informatics*, 25(9):3596–3607, 2021.
- Marie-Pier Gauthier, Jennifer H Law, Lisa W Le, Janice J N Li, Sajda Zahir, Sharon Nirmalakumar, Mike Sung, Christopher Pettengell, Steven Aviv, Ryan Chu, Adrian Sacher, Geoffrey Liu, Penelope Bradbury, Frances A Shepherd, and Natasha B Leighl. Automating access to real-world evidence. *JTO Clin. Res. Rep.*, 3(6):100340, June 2022.
- Akshay Goel, Almog Gueta, Omry Gilon, Chang Liu, Sofia Erell, Lan Huong Nguyen, Xiaohong Hao, Bolous Jaber, Shashir Reddy, Rupesh Kartha, Jean Steiner, Itay Laish, and Amir Feder. Lms accelerate annotation for medical information extraction, 2023.
- Javier González, Cliff Wong, Zelalem Gero, Jass Bagga, Risa Ueno, Isabel Chien, Eduard Oravkin, Emre Kiciman, Aditya Nori, Roshanthi Weerasinghe, et al. Trialscope: A unifying causal framework for scaling real-world evidence generation with biomedical language models. *arXiv e-prints*, pp. arXiv-2311, 2023.
- Yan Hu, Qingyu Chen, Jingcheng Du, Xueqing Peng, Vipina Kuttichi Kelothe, Xu Zuo, Yujia Zhou, Zehan Li, Xiaoqian Jiang, Zhiyong Lu, Kirk Roberts, and Hua Xu. Improving large language models for clinical named entity recognition via prompt engineering. *Journal of the American Medical Informatics Association*, pp. ocad259, 01 2024. ISSN 1527-974X. doi: 10.1093/jamia/ocad259. URL <https://doi.org/10.1093/jamia/ocad259>.
- Jenna Kefeli, Jacob Berkowitz, Jose M Acitores Cortina, Kevin K Tsang, and Nicholas P Tatonetti. Generalizable and automated classification of tnm stage from pathology reports with external validation. *Nature Communications*, 15(1):8916, 2024.
- Peter Lee, Sebastien Bubeck, and Joseph Petro. Benefits, limits, and risks of gpt-4 as an ai chatbot for medicine. *New England Journal of Medicine*, 388(13):1233–1239, 2023.
- Nelson F Liu, Kevin Lin, John Hewitt, Ashwin Paranjape, Michele Bevilacqua, Fabio Petroni, and Percy Liang. Lost in the middle: How language models use long contexts. *Transactions of the Association for Computational Linguistics*, 12:157–173, 2024.
- Jacqueline Miller, Laurie Hailer, and Susan Chapman. Cancer registrar workload and staffing study: Guidelines for hospital cancer registry programs. In *2024 Annual Research Meeting*. Academy-Health, 2024.
- Iman Mirzadeh, Keivan Alizadeh, Hooman Shahrokhi, Oncel Tuzel, Samy Bengio, and Mehrdad Farajtabar. Gsm-symbolic: Understanding the limitations of mathematical reasoning in large language models, 2024. URL <https://arxiv.org/abs/2410.05229>.
- National Cancer Registrars Association. Salary considerations for cancer registrars: 2022. <https://www.ncra-usa.org/Advocacy/Workforce/Salary-Considerations>, 2022. Accessed June 11, 2025.
- Mizuki Nishino, Jyothi P Jagannathan, Nikhil H Ramaiya, and Annick D Van den Abbeele. Revised recist guideline version 1.1: what oncologists want to know and what radiologists need to know. *American Journal of Roentgenology*, 195(2):281–289, 2010.

-
- Harsha Nori, Yin Tat Lee, Sheng Zhang, Dean Carignan, Richard Edgar, Nicolo Fusi, Nicholas King, Jonathan Larson, Yuanzhi Li, Weishung Liu, et al. Can generalist foundation models outcompete special-purpose tuning? case study in medicine. *Medicine*, 84(88.3):77–3, 2023.
- Sam Preston, Mu Wei, Rajesh Rao, Robert Tinn, Naoto Usuyama, Michael Lucas, Yu Gu, Roshanthi Weerasinghe, Soohee Lee, Brian Piening, Paul Tittel, Naveen Valluri, Tristan Naumann, Carlo Bifulco, and Hoifung Poon. Toward structuring real-world data: Deep learning for extracting oncology information from clinical text with patient-level supervision. *Patterns (N. Y.)*, 4(4):100726, April 2023a.
- Sam Preston, Mu Wei, Rajesh Rao, Robert Tinn, Naoto Usuyama, Michael Lucas, Yu Gu, Roshanthi Weerasinghe, Soohee Lee, Brian Piening, et al. Toward structuring real-world data: Deep learning for extracting oncology information from clinical text with patient-level supervision. *Patterns*, 4(4), 2023b.
- Ryan D Rosen and Amit Sapra. Tnm classification. In *StatPearls [Internet]*. StatPearls Publishing, 2023.
- Vivek A Rudrapatna, Atul J Butte, et al. Opportunities and challenges in using real-world data for health care. *The Journal of clinical investigation*, 130(2):565–574, 2020.
- Thomas Searle, Zina Ibrahim, James Teo, and Richard Dobson. Estimating redundancy in clinical text. *Journal of Biomedical Informatics*, 124:103938, December 2021. ISSN 1532-0464. doi: 10.1016/j.jbi.2021.103938. URL <http://dx.doi.org/10.1016/j.jbi.2021.103938>.
- Cliff Wong, Sheng Zhang, Yu Gu, Christine Moun, Jacob Abel, Naoto Usuyama, Roshanthi Weerasinghe, Brian Piening, Tristan Naumann, Carlo Bifulco, and Hoifung Poon. Scaling clinical trial matching using large language models: A case study in oncology, 2023.
- Wenxuan Zhou, Sheng Zhang, Yu Gu, Muhao Chen, and Hoifung Poon. Universalner: Targeted distillation from large language models for open named entity recognition, 2024.

10 SUPPLEMENTARY MATERIAL

Table S1. Oncology attributes and the associated event descriptors that can be defined as part of the attribute definition block in UMA prompt

Attribute	Descriptors	Definition	Extracted Example Values
Case Finding	cancer diagnosis	tumor histology	lung adenocarcinoma
	cancer diagnosis status	status of the diagnosis	positive, negative, suspicious, historical
	date	cancer diagnosis date	2016-12-15
PD-L1 Biomarker	biomarker measurement type	specifies PD-L1 IHC measurement type	CPS, TPS, expression
	biomarker variant	biomarker's variant or test value	10%, 5, High, T790M
Performance Status	performance status	performance status snippet	ECOG 1, KPS 90%
	performance status measurement type	the scale used for performance status	ECOG, KPS, Lansky
	performance status value	the value of the performance status	CPS, TPS, expression
Treatment	treatment	treatment name	pembrolizumab, carboplatin, radiation
	treatment date	treatment start date	2014-02-03
Response Progression	response	tumor response events	complete response, partial response, progressive disease, stable disease
	response disease	the disease or organ associated with the response	brain, lung, colon
	response disease type	the type of disease with regard to cancer	tumor, lymph node, or non-cancerous tissues
Primary Site Coarse	Primary Site Coarse	Body site of primary tumor	C50 (Breast), C34 (Lung)
Primary Site Fine	Primary Site Coarse	Body site of primary tumor	C50.4 (Upper-outer quadrant of breast)
Histology	Histology	Cell type of tumor	8046 (non-small cell lung cancer)
Clinical T	Clinical T	Clinical tumor staging	None, cT1, cT2, cT3, cT4
Clinical N	Clinical N	Clinical nodal staging	None, cN0, cN1, cN2b
Clinical M	Clinical M	Clinical metastatic staging	None, cM0, cM1
Pathologic T	Pathologic T	Pathologic tumor staging	None, pT1, pT2b
Pathologic N	Pathologic N	Pathologic nodal staging	None, pN0, pN1, pN2b
Pathologic M	Pathologic M	Pathologic metastatic staging	None, pM1

Table S2. Description of the test sets from Providence. Path. = Pathology. For performance status, we include the following note types: Progress Notes + Telephone Encounter + H&P + Consults + Discharge Summary + Assessment and Plan Notes + Plan of Care + Research Note + Treatment Plan

Attributes	# patients	# notes	# Attribute Occurrences	Note and Report Types	Tumor Types
PD-L1 biomarker	298	298	173	Path. Reports + Progress Notes	All
Performance Status	45	565	45	Progress Notes + Telephone Encounter...	All
Treatment	18	431	203	Progress Notes	Lung Cancer
Progression	70	243	27	Imaging Reports	Lung Cancer
Response	70	243	28	Imaging Reports	Lung Cancer
Case Finding	10,501	59,618	10,501	Path. and Imaging & Reports	All
Long-context Attributes	2,918	33,293	2,918	Path., imaging and surgical reports	All

Table S3. Number of patients, notes and per-patient counts in the Providence and Hopkins datasets for long-context attribute abstraction

	Providence	Hopkins
# of patients	2,918	592
# of notes (all)	33,293	7,555
# of imaging reports	21,936	6,221
# of pathology reports	11,357	1,334
# median per-patient tokens	3984	5352
# median per-patient notes	7	10
# median per-patient imaging reports	6	9
# median per-patient pathology reports	2	2

10.1 SHORT-CONTEXT ATTRIBUTE ABSTRACTION TASKS

We test UMA on six short-context attributes that can be understood and abstracted in the immediate context within a single note. Figure 1B shows the template for abstracting short-context attributes.

For the per-task configurations, we provide the attribute definitions according to Section 10. For the per-patient input block, we input each note separately, and then collect the outputs for each patient for the final postprocessing step. For evaluation, we attach patient ID as an additional key to each attribute occurrence and count as positive when all the keys and values of the attribute correctly match the groundtruth. We report precision, recall and F1. We obtain manual annotations and relevant patient notes from Providence Health.

PD-L1 PD-L1 protein expression is an important biomarker used to predict immunotherapy outcome as a high PD-L1 level may respond well to certain immune checkpoint inhibitor. Being able to extract the PD-L1 biomarker attribute can significantly facilitate the patient recruiting process in clinical trial matching. To configure the attribute definition block, we define the PD-L1 attribute by identifying two descriptors: the biomarker measurement types (eg. Combined positive score (CPS) or tumor proportion score (TPS)) and the biomarker variant descriptor that outputs the measurement values. To create the evaluation dataset, we manually curated 173 labels from 298 patients from the Providence data.

Performance Status Performance status is a standard clinical criterion used to assess a patient’s ability to carry out daily activities and is commonly required for eligibility in cancer clinical trials.

To construct the evaluation dataset, we manually labeled performance status in clinical notes from 45 patients in the Providence dataset. A single clinician performed the initial annotations. Model predictions were generated using the o3 model, and any discrepancies between model output and annotations were adjudicated by a second clinician.

The model was instructed to extract ECOG scores either from explicit documentation (e.g., “ECOG 2”) or, when absent, to infer the score based on narrative descriptions of functional status (e.g., self-care, ambulation, bed confinement). When both an explicit score and a functional description were present but inconsistent, the inferred score based on functional status was prioritized. If the note lacked sufficient information, the model returned “N/A.”

Treatment The treatment attribute is a fundamental attribute of patient data, providing critical information about the timing and nature of treatments a patient has received. This data is essential for various downstream applications, such as predicting treatment outcomes and matching patients to clinical trials, which often require participants with specific prior treatments. In the task configuration section of the template, we define two key descriptors for the treatment attribute: the date of treatment and the treatment name. To create the evaluation set, we leverage existing treatment metadata from Providence. However, we observed that this structured data does not always capture all the treatments mentioned in the reports. As a result, we reviewed and manually corrected the data from a randomly selected subset to create a gold-standard test set.

Response and Progression Response and progression are important attributes to assess the treatment outcome of a clinical trial. In general, response indicates that the patient is showing improvement with the treatment, while progression signifies a worsening of the patient’s condition. The response and progression attributes are extracted in one prompt. To provide the task-specific configurations in the template, we define response and progression based on the RECIST guideline (Nishino et al., 2010)². Specifically, we require LLM to list the specific response labels (choosing from: partial response, complete response, progressive disease or stable disease) and the corresponding response disease for each attribute occurrence. For each note, we collect the response attributes and progression attributes separately from the same LLM output: if there is an occurrence of partial response or complete response for a disease in the note, we assign a response label. If there is an occurrence of progressive disease event in the note, we have a progression label. We manually curated the labels which are divided into 261 train labels and 55 test labels (28 response labels and 27 progression labels).

Case Finding Case finding is a system for locating patients who is diagnosed at a particular time. Case finding is essential for ensuring that cancer registries provide comprehensive, accurate, and

²To curate the annotations from the reports, we relaxed the RECIST criteria to accommodate the level of details commonly available in standard follow-up radiology reports.

timely data, which is critical for research, public health planning, and improving patient outcomes. To extract the case finding attribute, we define the diagnosis time as the key descriptor in the attribute definition block of our template as the ultimate goal of the task is to identify the moment of cancer diagnosis. We evaluate case finding extraction with labels collected from the cancer registry following the method in Preston et al. (2023b). With around 50k train labels, we provide a supervised baseline BERT model that predicts a binary label of whether the diagnosis happens given the note date following the setup in Preston et al. (2023b).

10.2 LONG-CONTEXT ATTRIBUTE ABSTRACTION: CANCER STAGING

Cancer staging is a process used to determine the extent of cancer in the body. It involves the abstraction of multiple long-context attributes that requires a model to follow the rules and definitions set up in the lengthy clinical guidelines, and make inferences across multiple notes from the entire patient history. For example, tumor measurements from imaging reports must be correlated with pathology findings to confirm a primary tumor site, and understanding the timing of diagnosis and treatments is crucial for determining their relevance to clinical or pathological staging values. UMA can effectively address these challenges. In the task configuration part, we offer the flexibility to take in long clinical guidelines and provide summarization specific to each attribute. These guidelines include the International Classification of Diseases for Oncology (ICD-O) manual, the American Joint Committee on Cancer (AJCC) Cancer Staging Manual, and the Standards for Oncology Registry Entry (STORE) manual. These sources were structured via a semi-automated process using GPT-4 to organize and summarize guidelines relevant to a particular abstraction task. To configure the attribute definition block, we define the attribute as the main descriptor to be extracted and since cancer staging involves complex reasoning and grounding, we also define two additional descriptors including the model reasoning descriptor and the evidence descriptor that enforce the LLM to generate rationale and the supporting evidence (i.e. the piece of text from the patient note that supports the extracted attributes) before generating the attribute value. As to patient input, given the cancer staging attributes require reasoning over the patient history, we offer the solution to generate attribute-specific summaries from the patient history and pass the summaries into the patient input block. Alongside unstructured notes, we also provide the flexibility to incorporate other existing structured data such as treatment date. The previously extracted cancer staging attributes can also be chained for the best result. For example, we extract tumor site first and then we use the tumor site information to guide the extraction of the T/N/M attributes. Figure 1C shows the full instantiation of UMA for this case.

In this study on cancer staging, we focus on abstracting the following eight attributes that are key in the staging process.

Primary site coarse/fine-grained : The primary site attribute extracts the primary site of the tumor and we extract two attributes with different granularity. In the attribute definition block in our universal template, we define the primary site coarse attribute as the coarse-grained tumor site with a finite set of choices (eg. C34 for “Lung”). For the fine-grained primary site attribute, we instruct the model to extract a more specific location (eg. C34.1 for “Upper lobe of the lung”).

Histology Histology describes the type of cells or tissues from which the cancer originates. We define the task requirements in the attribute definition block and instruct the model to output the four-digit ICD-O-3 histology code.

Clinical T/N/M We follow the conventional TNM system in determining cancer staging (Rosen & Sapra, 2023). We first define the clinical staging attributes which describe staging results determined before treatment initiation. Specifically, we define clinical T (tumor) attribute as describing the size and extent of the primary tumor and it is a multi class classification task. Similarly, we define clinical N (nodule) attribute which describes the involvement of regional lymph nodes, and we define clinical M (Metastasis) as describing whether the cancer has metastasized. The exact definitions of the output values come from the attribute-specific summarization of the clinical guideline that lays out the detailed rules and requirements for determining the staging outcome. To prepare the patient input, we also pass in other structured data alongside the unstructured notes. For example, we pass in treatment date which is essential for guiding the LLM to extract staging information only from

records prior to the treatment date. We also input primary site attributes that we have previously extracted as additional structured data context to guide LLM to provide the correct staging results.

Pathologic T/N/M The pathologic T/N/M attributes have the same setup to clinical T/N/M apart from the different sources of staging information, allowing the use of staging information collected during treatment including excised tumor tissue.

Dataset and baselines Our primary dataset was obtained from Providence Healthcare where we collected electronic patient records and linked them to their cancer registry. We excluded cases lacking a pathology report within 30 days of the diagnosis date listed in the cancer registry. Additionally, patients with multiple primary cancer diagnoses were excluded from the study.

To provide a more comprehensive evaluation and test the generalization abilities of our approach, in addition to the data from Providence Healthcare, we collaborated with members of Johns Hopkins Medicine to compile a similar validation dataset from their cancer registry and patient records. This process involved collecting data from the cancer registry, integrating it with electronic patient records, and filtering based on the presence of a pathology report near the diagnosis date. Characteristics of the two datasets prepared for cancer staging evaluation are detailed in Table S3 and Figure S1. We note that in the Hopkins dataset, a patient generally has more imaging reports and the notes are usually longer. In addition to differences in clinical notes, the staging datasets have different distributions of primary tumor sites, shown in Figure S1. While the Providence dataset is dominated by breast cancer, the Johns Hopkins dataset has a much higher portion of lung, blood, pancreatic, and brain cancer.

To establish an upper bound performance from conventional methods, we train a supervised baseline using the dataset (with 23438 patients’ medical records as the train and dev set) and follow the methods described in Preston et al. (2023b). We modify the original tasks to make the evaluation more realistic by (1) including a "None" category for each prediction, allowing the model to indicate there is not enough information to make a prediction; (2) predicting standard four-digit histology codes; and (3) using the standard nodal staging instead of simplified N0/N+ classification. For the Hopkins dataset, we only have the test labels and we directly run the supervised model trained on the Providence dataset. For UMA, we provide a zero-shot setting and we use the same prompt template for the two datasets except for passing in different clinical guidelines that are used in Providence and Hopkins. As to the underlying LLMs for UMA, we use GPT-4 and GPT-4o as they are the most competitive LLMs as verified by the short-context attribute abstraction experiments. We report accuracy rather than F1 for all the tasks, because each patient will have a prediction for each attribute, even if the prediction is *None* (i.e. not enough information to determine).

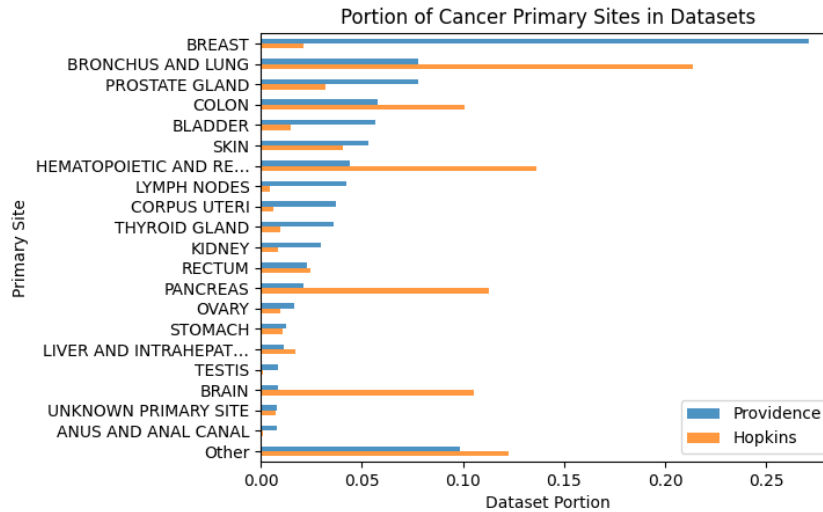


Figure S1. Distribution of primary sites in Providence and Johns Hopkins datasets.

Table S4. Testing UMA on short-context attribute abstraction tasks in oncology. We show zero-shot UMA with GPT-4o achieves overall F1 improvement compared with the conventional baseline approaches. For performance status, we also experimented with reasoning models such as o1 and o3 and have found further gains.

Patient Attributes	Approach	Precision	Recall	F1
PD-L1 biomarker	Heuristics	97.5	89.6	93.4
	UMA (GPT-4)	97.0 \pm 1.0	95.3 \pm 1.2	96.1 \pm 1.0
	UMA (GPT-4o)	97.7\pm0.8	98.8\pm0.6	98.3\pm0.6
Performance Status	Heuristics	53.3	53.3	53.3
	UMA (GPT-4)	74.1\pm2.6	74.1\pm2.6	74.1\pm2.6
	UMA (GPT-4o)	73.3\pm1.0	71.1\pm0.0	72.2\pm0.5
	UMA (GPT-o1)	81.3\pm3.5	77.1\pm1.3	79.1\pm2.4
	UMA (GPT-o3)	78.9\pm3.1	78.4\pm3.1	78.7\pm3.1
Treatment	Heuristics	85.0	85.0	85.0
	UMA (GPT-4)	83.4 \pm 4.1	89.3\pm4.2	86.2 \pm 3.0
	UMA (GPT-4o)	87.8\pm2.0	86.8 \pm 2.5	87.3\pm1.8
Progression	Supervised Model	75.9	81.5	78.6
	UMA (GPT-4)	67.3 \pm 5.6	100\pm0.0	80.3 \pm 4.0
	UMA (GPT-4o)	69.2 \pm 5.9	100\pm0.0	81.8\pm4.0
Response	Supervised model	68.4	92.9	78.8
	UMA (GPT-4)	67.7 \pm 6.1	89.4 \pm 4.6	76.9 \pm 4.5
	UMA (GPT-4o)	69.2 \pm 5.9	89.0 \pm 4.5	77.7 \pm 4.4
Case Finding	Supervised Baseline	88.5	94.3	91.3
	UMA (GPT-4)	86.9 \pm 0.3	89.8 \pm 0.3	88.3 \pm 0.2
	UMA (GPT-4o)	86.9 \pm 0.3	89.9 \pm 0.3	88.4 \pm 0.2
Average	SOTA baseline	78.1	82.8	80.1
	UMA (GPT-4)	79.4 \pm 3.3	89.7\pm2.2	83.7 \pm 2.6
	UMA (GPT-4o)	80.7\pm2.6	89.3 \pm 1.3	84.1\pm1.8

Table S5. Performance comparison (measured in accuracy) of supervised models and zero-shot UMA on the long-context cancer staging attribute abstractions in the Providence dataset. The supervised baseline is trained with the Providence train set.

	Supervised (trained from Providence)	UMA (GPT-4o)	UMA (O1)
Primary Site Coarse	92.6 \pm 0.5	93.2 \pm 0.5	93.6\pm0.5
Primary Site Fine	71.8\pm0.9	68.6 \pm 0.9	68.4 \pm 0.9
Histology	80.9\pm0.8	74.3 \pm 0.8	74.6 \pm 0.8
Clinical T	58.7\pm1.0	51.3 \pm 1.0	55.4 \pm 1.0
Clinical N	91.0 \pm 0.6	86.4 \pm 0.7	91.2\pm0.5
Clinical M	95.2\pm0.4	92.3 \pm 0.5	95.2\pm0.4
Pathologic T	55.0 \pm 1.0	75.4 \pm 0.8	77.5\pm0.8
Pathologic N	62.4 \pm 1.0	75.8 \pm 0.8	78.3\pm0.8
Pathologic M	93.8 \pm 0.5	94.1 \pm 0.5	96.0\pm0.4
Average	77.9 \pm 0.3	79.0 \pm 0.3	81.1\pm0.3

Table S6. Performance comparison (measured in accuracy) of supervised models (trained with the labels from the Providence data) and zero-shot UMA on the long-context cancer staging attribute abstractions in the held-out Johns Hopkins Medicine dataset where no training labels are available.

	Supervised (trained from Providence)	UMA (GPT-4o)	UMA (O1)
Primary Site Coarse	82.6±1.5	89.5±1.2	90.9±1.2
Primary Site Fine	67.5±1.9	71.6±1.9	72.6±1.8
Histology	59.8±2.0	61.2±2.0	60.7±2.0
Clinical T	49.8±2.1	55.8±2.0	54.7±2.1
Clinical N	59.7±2.0	68.0±2.0	76.0±1.7
Clinical M	83.0±1.6	83.5±1.5	89.1±1.3
Pathologic T	73.2±1.8	77.8±1.8	83.4±1.5
Pathologic N	52.7±2.0	78.1±1.8	85.4±1.4
Pathologic M	71.4±1.9	81.0±1.6	87.0±1.4
Average	66.6±0.8	74.0±0.7	77.7±0.7

Table S7. Average per-patient token usage and cost using O1 on the Johns Hopkins dataset

	Prompt	Completion	Reasoning	Cost (USD)
Primary Site Coarse	3 104	2 519	2 267	0.20
Primary Site Fine	2 490	3 288	2 910	0.23
Histology	4 608	2 777	2 513	0.24
Clinical T	10 310	12 911	11 981	0.93
Clinical N	2 387	2 359	2 195	0.18
Clinical M	2 743	2 851	2 606	0.21
Pathologic T	5 826	5 607	5 001	0.42
Pathologic N	3 559	2 567	2 300	0.21
Pathologic M	2 926	2 458	2 153	0.19
Sum	37 953	37 336	33 926	2.81

Summarization Prompt

Briefly summarize the given clinical document, specifically including information related to cancer diagnosis and staging such as:

- tumor information
 - detailed location
 - size
 - primary or metastatic
 - extent and structural invasion
- tumor tissue characteristics
 - tumor morphology, including histology, behavior, and grade
 - source, whether biopsy, resection, or cytology
- lymph node involvement
- explicit diagnosis or staging information
- treatment information, such as chemotherapy, radiation, or surgery

The title of the summary should give information about the procedure or observation being described.

In particular, include the following information for the specific note types below:

Imaging Reports: include the imaging modality, body site imaged, and purpose of the imaging

Pathology Reports: include the type of tissue or fluid being examined, including whether the tissue is from a biopsy or resection

For other note types, include the type and purpose of note.

Additional summarization instructions:

- Document the source of any tumor tissue, whether biopsy, resection, or cytology.
- If there is no relevant information, generate a title but leave the findings empty.

The output format is a JSON blob that contains the summary findings as well as evidence from the original note to support each finding. The format is given below:

```
{format_instruction}
```

If there is no relevant information, create the title but leave the findings as an empty list.

Figure S2. Prompt template for task-specific note-level summarization.